

# Cosmogenesis Backgrounds, Experiment Depth and the Solar Neutrino TPC

G. Bonvicini, A. Schreiner \*

Wayne State University, Detroit MI 48201

---

## Abstract

A Time Projection Chamber (TPC) is one of the promising candidates to perform unique measurements in solar neutrino physics. Its features will enable it to work at depths of the order of 2000 mwe. This paper describes an estimation of the expected cosmogenic background at different depths including also the background due to fission activation of the TPC material above ground.

*Key words:* solar, neutrino, detector

*PACS:* 26.65, 96.60.J

---

## 1 Introduction

A solar neutrino Time Projection Chamber (TPC) provides unique and very powerful information about solar neutrinos, their nuclear parents and their fluxes (electron and non-electron), which ultimately translates into better measurements of the neutrino mass and mixing parameters [1].

The TPC measures only  $\nu - e$  elastic scattering, and determines the electron direction and kinetic energy. This information allows reconstruction of the incident neutrino energy.

Directionality also allows to use only electrons recoiling away from the sun, effectively eliminating most background events. The rest of the background events is eliminated by subtracting a 12-hours delayed coincidence, very much the same way as the SuperKamiokande experiment can extract a clean solar

---

\* Corresponding author. Permanent address: Physics Dept., Wayne State University, Detroit MI 48201, USA. Tel.: +1-313-577-5067; Fax: +1-313-577-3932.

*Email address:* schrein@physics.wayne.edu (A. Schreiner).

neutrino sample mixed with a much larger non-directional background [2]. In that experiment, however, low recoil angle and large multiple scattering conspire to destroy any directional information that could help to determine the neutrino energy. The TPC considered here looks at events with large scattering angle and low multiple scattering [1].

This paper is written for the sole purpose of confirming that this detector can work at moderate depths. This has been the subject of much skepticism in public meetings, and besides the main results, consistency checks are offered. There are several advantages in working at moderate depths:

- Virtually all available underground sites can accommodate this detector, allowing us to concentrate on the aspects that really matter: low excavation costs, low radon, quality and quantity of dust contamination, and strong laboratory support.
- This detector will be housed in a gigantic hall. Low overburden reduces the civil engineering complexity.
- Very deep sites have unacceptable rock temperatures, making the assembly and operation more difficult and expensive.
- Moderate depths allow the plentiful observation of certain background events, which provide excellent calibration of the TPC performance. These include [3]:
  - $O(10^6)$  straight, minimum-ionizing cosmic rays per year, which allow a complete calibration of the electric field, gain, electronics amplification, electron lifetime, and diffusion, without a need for separate hardware and software. A TPC “without moving parts” minimizes failures and avoids costly and potentially contaminating accesses.
  - $O(10^5)$  delta rays above 100 keV per year. These have a well-known kinematic relation between the angle and energy of the delta ray, providing free and very accurate calibration of the detector resolution.

In section 2, we introduce concepts useful to the analysis. The main results are presented in section 3, divided into analyzes of cosmogenesis backgrounds generated above and below ground. Depths between 1500 and 3000 mwe are considered. In section 4, we cross check our results against other, published results and draw the conclusions.

## 2 Overview of the TPC and cosmogenesis

In the following, we consider a TPC whose parameters have been outlined in [3]. Briefly, as shown in Fig.1, it is a TPC of 4000 cubic meters volume, surrounded by a 1.5 meters of radiopure, hydrogen rich material (either plastic or water ice), which forms the inner shielding. Surrounding the inner shielding

are 30 centimeters of steel, forming the pressure vessel and outer shielding. The weight of the inner shield is 1.9 kilotons, and the weight of the iron is 3.6 kilotons. The last five centimeter thick layer of the inner shield, surrounding the TPC, weighs 59 tons. We mention it here because it is particularly helpful for instantly estimating self-shielded backgrounds (see section 2).

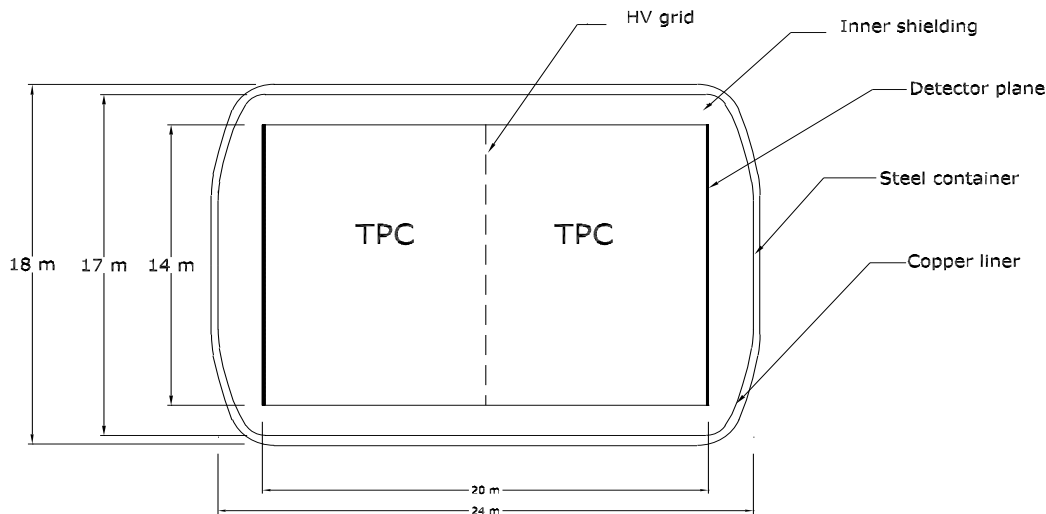


Fig. 1. Sketch of TPC cage and surroundings.

The TPC contains 7.6 tons of gas at ten atmospheres, and the gas is a mixture of helium (97%) and methane (3%), for a total methane weight of 840 kg. The TPC will also contain approximately 100 kg of electrodeposited copper and 2 kg of sense wires. With these conditions, 14 meters of gas (the diameter of the chamber) represent approximately 0.14 Compton interaction lengths, indicating that roughly one in seven 1 MeV gamma rays entering the chamber will interact with the gas.

We have discussed elsewhere [3,4] that recoiling electrons will generate a track of 9 cm length for 100 keV electrons and of 1.8 m for 600 keV electrons. The maximum drift time is 8.3 milliseconds, so that the TPC snaps an electronic picture of the gas volume 120 times per second. Whenever an event is encountered, a time interval around the event of  $\pm 9$  msec is considered for vetoing.

The signal (a single electron) is readily simulated by  $\beta$  radiation inside the active volume, and  $\gamma$  radiation from any source, generating a Compton scattering inside the chamber.

When looking at the volume distribution, the TPC occupies about 62% of the

volume in Fig.1. Most cosmic rays will track through the sensitive volume and provide a direct veto that eliminates all short-lived radionuclides as well as neutrons, which thermalize and are absorbed in about 0.1 msec in the inner shield. About 25% of cosmic rays crossing the steel shell will not cross the active volume and all types of radioactive backgrounds produced by them will have to be considered.

When looking at the weight distribution, however, the active volume of the TPC only has a 0.13% share of the total weight. Cosmogenesis backgrounds produced outside the active volume have a very small chance of interacting with the gas.

In [1], it was found that background rates of around 600 events per day, above 100 keV and before directional cuts, result in a non-dominant background subtraction error over two years of data taking. Over a longer period of time, even background rates at the level of one thousand events per day will not drastically affect the final precision of the experiment.

## 2.1 Cosmic generation of radionuclides

At any given depth, the quantity of a particular long-lived daughter  $i$ , generated in a given sample of mother nuclei  $j$ , can be described by a charging capacitor law

$$N_c(t) = \epsilon_{ij}(h)\tau(1 - e^{-t/\tau}) \quad (1)$$

where  $\tau$  is the daughter nuclide lifetime. The variable  $\epsilon_{ij}(h)$  carries all the information about the reaction probability,

$$\epsilon_{ij}(h) = \langle \sigma_{ij}(h) \rangle N_t \Phi(h). \quad (2)$$

Here  $N_t$  is the number of target nuclei,  $\Phi(h)$  the depth-dependent flux, and  $\langle \sigma_{ij} \rangle$  the cross-section for the process, averaged over the depth-dependent spectrum,

$$\langle \sigma_{ij}(h) \rangle = \frac{1}{\Phi(h)} \int dE \sigma_{ij}(E) \frac{d\Phi(E, h)}{dE}. \quad (3)$$

The values of  $\epsilon_{ij}(h)$  for dominant reactions are given in table 1.

The cross section depends strongly on the depth. Besides the overburden attenuation, nuclide activation is dominated by hadronic showers at sea level

reaction	$\epsilon_{ij}(0\text{mwe}),$ $\text{ton}^{-1}\text{day}^{-1}$	$\epsilon_{ij}(1500\text{mwe}),$ $\text{ton}^{-1}\text{day}^{-1}$	$\epsilon_{ij}(3000\text{mwe}),$ $\text{ton}^{-1}\text{day}^{-1}$
Fe $\rightarrow$ <sup>54</sup> Mn	410000	15	0.73
Cu $\rightarrow$ <sup>60</sup> Co	91000	3.2	0.16
C $\rightarrow$ <sup>7</sup> Be	19000	0.61	0.03
C $\rightarrow$ <sup>11</sup> C	-	2.4	0.12

Table 1

The activation probabilities  $\epsilon_{ij}(h)$ , for significant reactions and at various depths.

( $h = 10.33$  meters of water equivalent, mwe), by muon capture at intermediate depths and by fast muons at all depths below 100 mwe [5].

The activity during charge-up is

$$A_c(t) = \epsilon_{ij}(h)(1 - e^{-t/\tau}). \quad (4)$$

and after a long time one obtains:

$$N_c(\infty) = \epsilon_{ij}(h)\tau, \quad A_c(\infty) = \epsilon_{ij}. \quad (5)$$

For a sample that is charged up at the surface and taken deep underground, the discharging capacitor equations hold:

$$N_d(t) = N_0 e^{-t/\tau}, \quad A_d(t) = \frac{N_0}{\tau} e^{-t/\tau}. \quad (6)$$

$N_0$  is, in all practical cases, close to  $N_c(\infty)$ . It can be reduced by up to two orders of magnitude for materials which are mined or taken deep underground, and are exposed to surface radiation during transportation or processing before storing underground again.

Cosmic fluxes, their energy and angular dependence were kindly provided by E. Nolte [5]. Dr. Nolte provided us also with the measured cross sections for nuclide production by fast muons, and the measured muon capture cross sections to estimate this source of backgrounds as well [5].

## 2.2 Cross section approximations

The following approximations were used when parameterizing nuclear cross sections. In processes involving a nucleus and an electromagnetic particle such

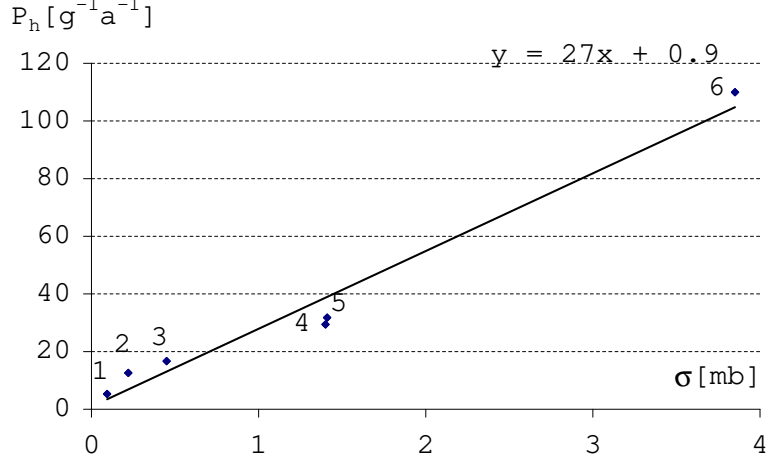


Fig. 2. Cross sections for nuclide production by 190 GeV muons versus rates of nuclide production by cosmic hadrons above ground. The reactions are labelled as follows:  $O \rightarrow ^{10}Be$  (1),  $S \rightarrow ^{26}Al$  (2),  $O \rightarrow ^{14}C$  (3),  $Ca \rightarrow ^{36}Cl$  (4),  $Si \rightarrow ^{26}Al$  (5),  $Fe \rightarrow ^{53}Mn$  (6).

as a muon, electron, or photon most activation occurs by exciting the giant dipole resonance through the exchange of a quasi-real 17 MeV photon. The resonance area is roughly proportional to the product of the nucleus charge  $Z$  and nucleus atomic number  $A$ . The resonance decays predominantly into a heavy nucleus and a nucleon. If the total resonant cross section is known, we multiply it by two to obtain an upper limit on total or partial activities where needed.

According to [5], the total radionuclide production cross section is assumed to depend on energy as:

$$\sigma(E) = \sigma_0 E^{0.75}. \quad (7)$$

The energy dependence includes secondary production by bremsstrahlung photons and high energy delta rays.

As will be shown in section 3, activation by cosmic rays at sea level is the dominating contribution to our backgrounds. Since the hadronic spallation cross sections of interest are not 100% measured [6], we estimated the missing cross sections using Fig.2, which plots the muon-nuclide cross sections, all known, against the cosmic hadron-nuclide production rates [6], not all known.

### 2.3 Compton absorption length

The volume-large TPC is surrounded by some 4 mwe of passive material (see Fig.1). This material is self-shielded, meaning that its thickness  $L$  is much

greater than the Compton absorption length  $\lambda$ , and only a very small fraction of the gamma rays produced within the device enters the active volume.

Under the conditions in which the inner shield is self-shielded, yet is thin compared to the dimensions of the TPC, the fraction  $f$  of gamma rays entering the TPC, can be estimated analytically:

$$f = \frac{1}{2L} \int_0^1 d \cos \theta \int_0^\infty dx e^{-x/\lambda \cos \theta} = \frac{\lambda}{4L} \quad (8)$$

where  $x$  is the distance between the origin point of the emitted photon and a TPC wall and  $\theta$  is the emission direction angle with respect to the perpendicular of this wall.

The factor of 1/2 in front of the right hand side of the equation takes into account those gamma rays that point away from the TPC. The result, by no means new, is displayed for two reasons: first, it makes very clear that radiopurity near the TPC is of paramount importance, and second, it allows for a quick cross check of more complex simulations by reducing the backgrounds to those originating from a smaller, known fraction of the shield.

The real life attenuation length of gamma rays originating outside the TPC involves also geometric factors and energy cuts (once a photon energy falls below 200 keV, it cannot generate a candidate). They have been calculated with GEANT and are shown in Fig.3.

#### 2.4 Radionuclides of interest

Considering the activation of inner shielding and gas, all daughters of C, He, and possibly O (if different type of inner shielding is chosen) need to be considered. No radionuclide has a half-life exceeding two months, meaning that activation above ground decays away during any reasonable construction and assembly time. The light radionuclides and their radioactivity parameters are shown in table 2.

For the steel shielding and copper strips, we also need to consider isotopes with half-lives exceeding several months (see table 3). These are activated at the surface.

### 3 Results.

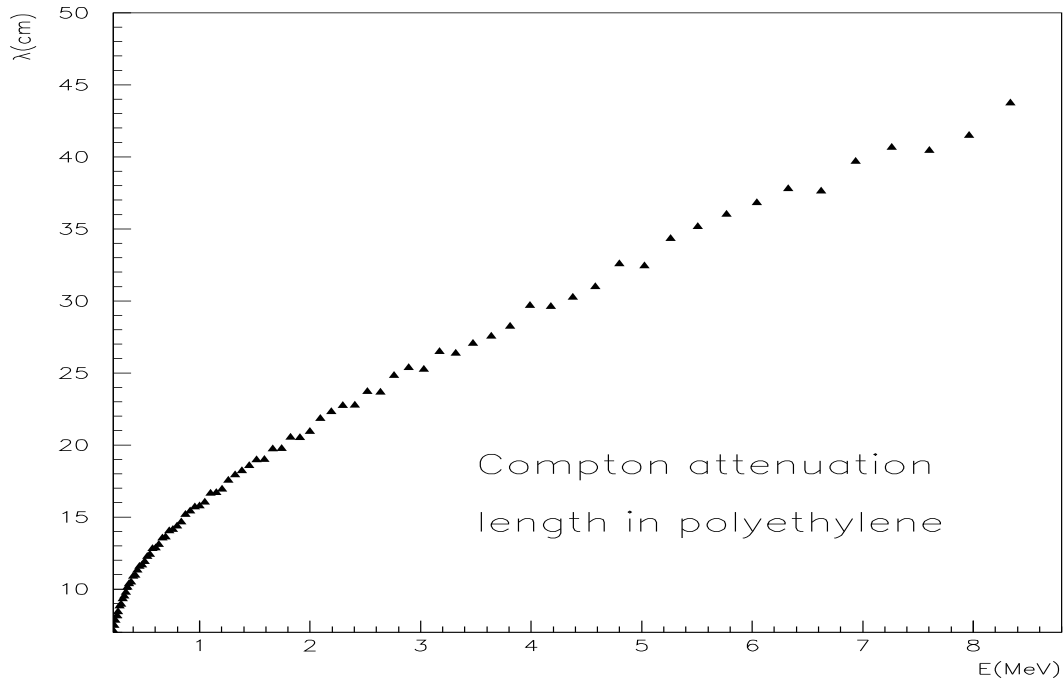


Fig. 3. GEANT Photon Compton absorption length in polyethylene ( $\rho = 1 \text{ g/cm}^3$ ) as a function of photon energy, and for a photon cutoff of 200 keV, as described in the text.

### 3.1 Above ground activation

There is no long-term above-ground activation of the inner shield or gas, as all possible daughters have half-lives well below one year. The two components that may be activated with long-lived radionuclides are the steel vessel and the copper strips and grids. We combine the tables of the preceding section to produce table 4, which evaluates the total rate of photons and background rates from the corresponding components. The above ground exposure time was chosen to be infinite.

We find already the largest background from  $^{60}\text{Co}$  activated in the copper immediately after being taken underground. A two year wait cuts the background down to 4000 events per day. However, copper will be electrodeposited on plastic to produce both strips and the various HV grids. Electrodeposition will probably strongly reduce most radio-impurities, including certainly cobalt. It should also be mentioned that tracks originating in the detector plane will look anomalous (the track beginning will be recorded by a single wire or strip, for example).



nuclide	half-life	$\gamma$		$\beta$	
		avg. E , MeV	intensity	avg. E, MeV	intensity x charge
$^6\text{He}$	0.8s			1.5	-1
$^8\text{He}$	0.12s	0.98	0.84	4	-1.84
$^8\text{Li}$	0.8s			6.2	-1
$^7\text{Be}$	53.3d	0.48	0.1		
$^{11}\text{Be}$	13.8s	2.1	1	1	-1
		5	2.13		
		7	2.7		
$^8\text{B}$	0.77s			6.7	+1
$^9\text{C}$	0.126	2.3	0.4	7	+1
$^{10}\text{C}$	19.2s	0.72	1		
$^{11}\text{C}$	20.39m			0.386	+1
n	0.1ms	2.2	1		

Table 2

Radionuclides produced in carbon target and their decay modes. Only long-lived nuclides dominantly produced are listed. Where the activity is  $\beta^+$ , two extra photons of energy 0.511 keV for each  $\beta^+$  are always implied.

### 3.2 Underground activation: TPC gas

Table 5 shows the activity in the TPC gas at four depths varying from 1500 to 3000 mwe. As can be seen, a  $^{11}\text{C}$  component dominates, however the backgrounds are still a few orders of magnitude below the expected TPC backgrounds of a few hundred events per day. Hydrogen is inert from a cosmogenesis point of view, while He contributes a modest tritium background on which we do not trigger.

### 3.3 Underground activation: inner shield

Table 6 shows the activity in the inner shield at four depths varying from 1500 to 3000 mwe. The table considers the cosmic rays which enter the TPC (all the short-lived radionuclides are removed).

The cosmic rays whose total induced activity needs to be considered are those which do not enter the TPC and are not vetoed. Their total contribution to

nuclide	half-life	$\gamma$		$\beta$	
		avg. E, MeV	intensity	avg. E, MeV	intensity x charge
$^{46}\text{Sc}$	84d	1	2	0.11	-1
$^{47}\text{Sc}$	3.3d	0.16	0.6	2	-1
$^{48}\text{V}$	16d	1.1	2	0.29	+0.5
$^{51}\text{Cr}$	28d	0.32	1		
$^{52}\text{Mn}$	5.6d	0.8	1.9	0.24	+0.3
		1.4	1		
$^{53}\text{Mn}$	3.7e6y	0.6	1		
$^{54}\text{Mn}$	312d	.83	1		
$^{56}\text{Co}$	77d	0.84	1	0.6	+0.19
		1.2	0.8		
		1.7	0.16		
		2.5	0.17		
$^{59}\text{Fe}$	44d	1.1	1	0.11	-1
$^{57}\text{Co}$	272d	0.12	1		
$^{58}\text{Co}$	71d	0.8	1	0.2	+0.15
$^{60}\text{Co}^{5+}$	5.3y	1.2	2	0.1	-1

Table 3

Radionuclides produced in the steel shielding and the copper strips and grids. Only long-lived nuclides produced dominantly are listed. Where the activity is  $\beta^+$ , two extra photons of energy 0.511 keV for each  $\beta^+$  are always implied.

target	$R_\gamma(t = 0)$ day $^{-1}$	$R_b(t = 0),$ day $^{-1}$	$R_b(t = 2y)$ day $^{-1}$
plastic	$3.5 \cdot 10^5$	3900	0.27
Cu	$8.2 \cdot 10^4$	8000	4000
Fe	$2 \cdot 10^7$	80	15

Table 4

Expected total rate of gamma emission immediately after installation due to activation of the TPC components by the cosmic flux above ground,  $R_\gamma(t = 0)$ , and background rate caused by this emission at the beginning,  $R_b(t = 0)$ , and two years later,  $R_b(t = 2y)$ .

depth, mwe	isotope	$R_\beta$ , day <sup>-1</sup>
1500	<sup>6</sup> He	0.029
	<sup>8</sup> He	0.0038
	<sup>11</sup> Be	0.0041
	<sup>8</sup> B	0.013
	<sup>9</sup> C	0.0085
	<sup>11</sup> C	1.6
	total	1.7
2000	total	0.53
2500	total	0.2
3000	total	0.083

Table 5

Background rate due to activation of methane in the gas by fast muons. Since the photon interaction probability is small, only  $\beta$ -emitters are included.

the background is related via Eq. (8) to the number of cosmic rays which cross the inner  $\lambda/4$ -thick layer of plastic but avoid the TPC. These are approximately 0.2% of the total cosmic rays crossing the TPC. We conclude that the contribution from non-vetoed short-lived species is negligibly small.

### 3.4 *Underground activation: copper and steel*

Table 7 shows the activity in the copper and the steel. As can be seen, this contribution is much smaller than from the inner shield.

### 3.5 *Underground activation: muon bremsstrahlung and muon capture*

The energy deposited by fast muons in our device increases by a factor of 1.7, to  $10^5$  GeV per day (1500 mwe), when bremsstrahlung is taken into account. At 3000 mwe, the factor and deposited energy are 2.2 and  $10^4$  GeV per day, respectively. The average photon energy (energy weighted) is approximately 100 (at 1500 mwe) to 150 GeV (at 3000 mwe). The average photon energy above 200 keV varies from 15 (at 1500 mwe) to 20 GeV (at 3000 mwe). Because of the  $Z^2$  dependence of bremsstrahlung, about 97% of the photons are emitted in the iron.

depth, mwe	isotope	$R_{emit}$ , day <sup>-1</sup>	$R_{ent}$ , day <sup>-1</sup>	$R_{int}$ , day <sup>-1</sup>
1500	<sup>8</sup> He	< 7.4	< 0.19	< 0.016
	<sup>7</sup> Be	80	1.6	0.17
	<sup>11</sup> Be	< 40	< 2.2	< 0.067
	<sup>8</sup> B	49	0.97	0.11
	<sup>9</sup> C	58	0.91	0.085
	<sup>10</sup> C	380	9	0.83
	<sup>11</sup> C	6300	130	13
	total	7000	140	15
	n	3900	140	3.3
2000	total	2200	45	4.8
2500	total	850	17	1.8
3000	total	350	7.1	0.75

Table 6

Total rate of emitted photons due to activation of the plastic inner shield by fast muons. The labelling is following:  $R_{emit}$  is the rate of emitted photons,  $R_{ent}$  the number of photons entering the TPC and  $R_{int}$  the number of photons interacting with the TPC gas. All short-lived radionuclides are removed.

depth, mwe	1500	2000	2500	3000
$R_{Fe}$ , day <sup>-1</sup>	$1.9 \cdot 10^{-3}$	$6.6 \cdot 10^{-4}$	$2.3 \cdot 10^{-4}$	$3.5 \cdot 10^{-5}$
$R_{Cu}$ , day <sup>-1</sup>	0.063	0.021	0.0078	0.0032

Table 7

Cosmogenic background caused by fast muons in the steel shielding and the copper strips and grids.

The total number of photons between 200 keV and 10 MeV is about 1000 (at 1500 mwe) to 50 (at 3000 mwe) per day, and they are emitted nearly parallel to the muon. In practice, simulations showed that this source of backgrounds contributes less than 0.1 candidate events per day at any depth.

Muon capture at these depths ranges from 0.03/ton/day (1500 mwe) to 0.002/ton/day (3000 mwe). These numbers are at least two orders of magnitude below those provided in table 1 and are negligible.

#### 4 Cross checks and conclusions

#### 4.1 Cross checks

There are ways to roughly cross check our results. If radiopurity is expressed in  $^{238}\text{U}$  equivalent purity, BOREXINO purity needs are about  $10^{-16}$  g/g [7] and less than ten events per day. In the case of the TPC, the cage needs to have a purity of  $10^{-13}$  g/g [3] and less than 600 events per day (the two numbers do not scale the same way because the cage weighs less than the BOREXINO inner detector, and because only a fraction of the gammas originating in the cage will interact in the TPC volume).

If BOREXINO would observe negligible backgrounds at 4500 mwe (1200 mwe below its current location), then the TPC will observe negligible backgrounds at roughly 1200 mwe, if scaled by purity, and at 2000 mwe, if scaled by number of events.

#### 4.2 Conclusions

The TPC has a unique set of properties amongst solar neutrino detector.

- (1) the active volume occupies 62% of the total device, but weighs only 0.1% of the total weight. The active volume intercepts a large fraction of the cosmic rays and most short-lived radionuclides are simply vetoed by the observable muon track.
- (2) it distinguishes events of multiplicity two or more from events of multiplicity one.
- (3) its active volume is virtually free of any significant cosmogenesis backgrounds. Cosmogenesis backgrounds come from the surrounding materials, which are self-shielded.
- (4) the TPC directional capability further eliminates most events not pointing at the sun, and subtracts statistically the remainder.

All of the characteristics above combine to give a detector virtually immune of cosmogenesis backgrounds at depths as low as 1500 mwe.

The largest long-term backgrounds found by this analysis were from copper and steel activated at the surface (which are independent of depth). Two lessons are to be learned from this analysis. First, copper will have to be electrodeposited, a procedure known to suppress backgrounds by at least a few orders of magnitude. In particular, electrodeposition virtually eliminates  $^{60}\text{Co}$  [8]. Second, during the R&D phase, there will be of order 0.5 meters of inner shielding, and the backgrounds should be dominated by  $^{54}\text{Mn}$  (after the R&D device is adequately shielded from the surrounding rock). There will be a premium in obtaining steel that has been "sheltered" from cosmic radiation.

In the final detector,  $^{54}\text{Mn}$  is taken care of by increasing the thickness of the inner shield by 0.5 meters (originally [3] a one meter thick inner shield was considered).

In practice, the TPC depth is not limited by backgrounds, but rather by dead time, surface charging and future applications for the TPC. Civil engineering needs to be assessed too to evaluate the cost of a very large hall as a function of depth.

As discussed above, each cosmic event vetoes 1.8% of a second, therefore it is advisable not to build the TPC above the depth where the cosmic muon rate is 1 Hz (approximately 1900 mwe).

Surface charging has been discussed in [3]. The advantages in building a TPC with insulating walls are better electrostatic stability and better control of the materials. The exact limit depends on the final choice of plastic and the safety factor above the charge-up limit. For acrylic it is probably advisable not to go above 2000 mwe, whereas a plastic as conductive as polyethylene would not be charged up under any realistic circumstances.

Future applications of the TPC may include dark matter searches, where low-energy nuclear recoil (roughly 20 keV) is the signature for dark matter interactions. The signature is non-directional, and the recoil energy is proportional to the nuclear mass of the target. In practice one tries to see a change in the very low energy spectrum when the gas nuclear mass changes (*e.g.*, varying the gas from helium to carbon, then to neon, argon, xenon). The lack of directional information, plus varying cosmogenesis backgrounds, will perhaps provide the most stringent constraints on depth.

### 4.3 Acknowledgements

We are particularly indebted to R. Brodzinski and E. Nolte. Dr. Brodzinski pointed out that backgrounds would probably be dominated by above ground activation, and provided information and criticism that was helpful throughout the paper. Prof. Nolte provided an early version of his soon-to-be published paper which provided the backbone for all the calculations and results presented in this paper.

## References

- [1] G. Bonvicini *et al.*, hep-ph/0109199, Contributed to Snowmass 2001, The Future of Particle Physics.

- [2] J. Boger *et al.*, Nucl. Instr. Meth. A449: 172,1999
- [3] G. Bonvicini, D. Naples and V. Paolone, hep-ex/010932, submitted to Nuclear Instruments and Methods.
- [4] E. Cheu, Tracking Studies, Solar Neutrino TPC Internal memo.
- [5] E. Nolte, private communications.
- [6] J. Stone *et al.*, Nucl. Instr. and Meth. B 92 (1994) 311; K. Nishiizumi *et al.*, J. Geophys. Res. 94 (1989) 17; K. Nishiizumi *et al.*, J. Geophys. Res. 101 (1991) 22,225; A. J. T. Jull *et al.*, Nucl. Instr. and Meth. in Phys. Res. B 92 (1994) 308; D. Lal and A. J. T. Jull, Nucl. Instr. and Meth. in Phys. Res. B 92 (1994) 291; F. M. Phillips *et al.*, Geophys. Res. Lett. 23 (1996) 23,949. J. M. Evans *et al.*, Nucl. Instr. and Meth. B 123 (1997) 334; B. Heisinger, Diploma thesis, Technical University of Munich, Germany (1994).
- [7] C. Arpesella *et al.*, hep-ex/0109031, submitted to Astropart. Physics.
- [8] R. Brodzinski, private communications.